

Optical Frequency Domain Reflectometry for High Density Multiplexing of Multi-Axis Fiber Bragg Gratings

Stephen Kreger, Sean Calvert, Eric Udd

Blue Road Research
376 NE 219th Ave
Gresham, OR 97030

ABSTRACT

An interferometric fiber grating interrogation system utilizing a depolarized Erbium ring laser was used to interrogate transversely strained gratings written through the polyimide coating with 1 mm spatial resolution, and the interferometric results were compared to waveforms taken using a broadband source and OSA.

INTRODUCTION

Many aerospace and civil structure monitoring applications could benefit from high density strain sampling density over a fiber length of up to hundreds of meters. Recently NASA Langley demonstrated the ability to multiplex 750 low reflectance fiber grating sensors in a single line for a wing structure ground test. The technology¹⁻³ (termed optical frequency domain reflectometry, or OFDR) used to support this test employed a tunable laser to sample low reflectance fiber gratings and interferometric methods to separate out overlapping spectral signatures. Blue Road Research has demonstrated the ability of fiber optic grating sensors to measure multi-axis strain^{4,5}, temperature, pressure⁶, corrosion⁷ and moisture. Combining large scale multiplexing with these various sensor types will enable comprehensive structural health monitoring over the entire vehicle or structure lifetime.

BACKGROUND

Wavelength multiplexing of a large numbers of high reflectivity fiber gratings is limited by shading effects. Employing a light source with larger spectral band is useful up to a point, but usually results in increased system cost and complexity. OFDR circumvents this optical bandwidth limitation to multiplexing by allowing temporal frequency discrimination between grating reflection signatures. As shown in Figure 1, the optical system is configured so that laser light reflected from a reference mirror interferes with the grating reflection. The interference produces a sinusoidal detector current signal I_D that has a phase term dependent

on the distance L between the reference mirror and the grating, the wavelength of light λ and the core index of refraction n :

$$I_D \propto \cos\left(\frac{4\pi nL}{\lambda}\right). \quad (1)$$

The frequency f_D of this sinusoidal signal is given by:

$$f_D = \frac{2nL d\lambda/dt}{\lambda^2}, \quad (2)$$

where $d\lambda/dt$ is the laser scan rate. Since the frequency of the detector current is proportional to the distance from the reference mirror, a Fourier transform of the detector signal gives the locations of each fiber grating. With the knowledge of the sensor locations, the detector signal can be passed through narrow band frequency filters in order to separate out spectral information from individual grating sensors even if the sensors occupy the same wavelength space. This technique requires, however, that the grating reflectivity must be relatively weak so that gratings at the same wavelength farther down the same string can still be illuminated and to prevent multiple reflections from adjacent gratings from producing spurious signals.

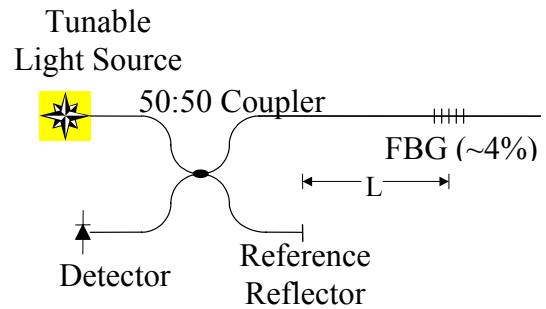


Figure 1. Basic OFDR High Density Fiber Grating Strain Sensing System

Embedding fiber gratings in structures is often desirable not only to better protect the sensing fiber, but also to allow measurement of strains transverse to the fiber in addition to axial strains. In general, fiber grating spectral reflections have two polarization eigenmodes, each aligned with the fiber core birefringence axes. Slight core ellipticity and nonuniform residual strains typically result in fiber grating peak separations of several pm

even in high quality single mode telecom fiber, and typically exceed several hundred pm in polarization maintaining fiber. Transverse loading of the fiber can also result in large peak separations between the polarization modes of a single grating. The shift in wavelength $\Delta\lambda$ of Bragg grating reflection peaks polarized in the x and y directions orthogonal to the fiber axis (z) in response to strain ε and temperature T can be expressed as:

$$\frac{\Delta\lambda_x}{\lambda_o} = \left(1 - \frac{n_o^2}{2} p_{12}\right) \varepsilon_z - \left(\frac{n_o^2}{2} p_{12}\right) \varepsilon_y - \left(\frac{n_o^2}{2} p_{11}\right) \varepsilon_x + \left(\frac{1}{n_o} \frac{dn_o}{dT} + \frac{n_o^2}{2} (p_{11} + 2p_{12}) \alpha\right) \Delta T \quad (3)$$

$$\frac{\Delta\lambda_y}{\lambda_o} = \left(1 - \frac{n_o^2}{2} p_{12}\right) \varepsilon_z - \left(\frac{n_o^2}{2} p_{12}\right) \varepsilon_x - \left(\frac{n_o^2}{2} p_{11}\right) \varepsilon_y + \left(\frac{1}{n_o} \frac{dn_o}{dT} + \frac{n_o^2}{2} (p_{11} + 2p_{12}) \alpha\right) \Delta T \quad (4)$$

In the above equations, p_{ij} are components of the strain-optic tensor, n_o is the effective index of the mode propagating in the core, λ_o is the center wavelength of the grating in the unstrained state, and α is the thermal expansion coefficient. For a purely axial strain change, and assuming that the material surrounding the fiber is much less stiff than fused silica, $\varepsilon_y = \varepsilon_z = -\nu\varepsilon_x$, where ν is Poisson's Ratio. In this case both peaks will shift by the same amount:

$$\frac{\Delta\lambda_{y,z}}{\lambda_o} = \left(1 - \frac{n_o^2}{2} (p_{12}(1-\nu) - \nu p_{11})\right) \varepsilon_x \quad (5)$$

If transverse strain is limited to the y-direction and we again assume that the material the fiber is embedded in is much less stiff than fused silica so that $\varepsilon_x = \varepsilon_z = -\nu\varepsilon_y$, peak separation is a linear function of the transverse strain:

$$\frac{\lambda_y - \lambda_z}{\lambda_o} = \frac{n_o^2}{2} (p_{12} - p_{11})(1 + \nu) \varepsilon_y \quad (6)$$

From a typical germanosilicate optical fiber $p_{12} = 0.252$, $p_{11} = 0.113$, $n_o = 1.46$, and $\nu = 0.17$.

EXPERIMENTAL SET-UP AND RESULTS

A straight-forward approach to using OFDR to measure axial and transverse strains is to only use pm fiber in the vicinity of the gratings, and to use a depolarized tunable laser source. To demonstrate the feasibility of this approach Blue Road Research obtained low reflectivity gratings in pm fiber, built test fixtures to apply transverse loads to the gratings, built a custom tunable laser, and assembled instrumentation to scan the laser and read out the individual gratings. An Erbium fiber ring cavity laser design was chosen because of its ease of construction, potential for the long coherence length

necessary to generate interference between widely space reflecting elements, as well as it's lack of polarizing elements in the laser cavity so that the laser output is highly depolarized and thus illuminates each polarization mode of the gratings regardless of orientation and fiber birefringence.

The Erbium fiber ring laser cavity design, similar to a design intended for telecommunications metrology applications,⁸ used for this demonstration is depicted in Figure 2. Light from a 980 nm pump laser diode is depolarized and injected into the cavity ring through a wavelength division multiplexing (WDM) coupler. The 980 nm light pumps a 3 m length of Erbium doped fiber, which re-emits the light over a range of 1520 to 1575 nm. A tunable etalon filter with a free spectral range of 50 nm and full width at half maximum of 0.2 nm passes only the selected wavelength through a 30 dB isolator. A coupler with only 5% cross-over insures strong levels of feedback in the ring. The output is passed through another WDM coupler to strip out any remaining 980 nm light, and through another 30 dB isolator to prevent back reflections from destabilizing the laser. The resulting laser output remained above 0.5 mW over a 40 nm tuning range, and could scan the range at rates up to 200 Hz. The coherence length of approximately 20 cm indicated a linewidth of approximately 0.01 nm. This coherence length is substantially less than that necessary for a practical system, but was sufficient for this demonstration. Previous work with Er-doped fiber ring cavity lasers has shown that coherence lengths of over 100 km are possible.⁹

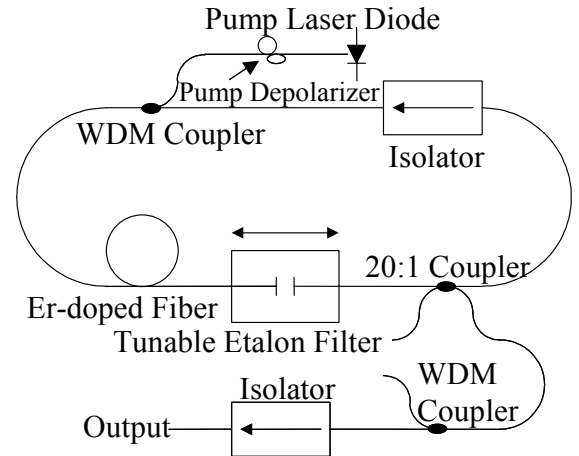


Figure 2. Tunable Erbium Fiber Ring Laser Design

The gratings used in this demonstration were written in polyimide-coated telecom grade polarization maintaining fiber through the polyimide coatings.¹⁰ This approach avoids having to strip and recoat the fiber, and thus better preserved the structural integrity of the fiber and reduced fabrication costs. The gratings were centered between 1551 and 1552 nm and had peak widths of 1.2 ± 0.1 nm full width at half maximum. Since the separation between reflection peaks polarized along the eigen-axes

of the fiber due to the fiber birefringence was only 0.45 nm, only a single peak was evident in the reflection profile. The unusually wide spectral width of the gratings was due to their short physical length of only 0.75 mm. Peak reflectivities were 23%, 9.3%, and 5.5%, and the gratings were labeled as Red, Green, and Blue, respectively.

Transverse loading fixtures, depicted in Figure 3, were designed and built to independently vary the transverse load on three nearby gratings until the peak separation became obvious. The gratings were separated from each other and oriented with the stress rods in the horizontal plane so that the peaks would separate further with increasing vertical loading, and the load was adjusted until the peak separation reached approximately 2 nm. The polyimide coating was left on the fiber for these tests. Using calibration data from previous diametrically opposed plate loading tests, we calculated that the load per unit length on the fibers was approximately 22 N/mm. The grating spectra were recorded before and after transverse loading using a broadband ASE source and an optical spectrum analyzer; Figure 4 shows the reflection spectra taken of grating “Blue”. The separation between Red and Green gratings was 35.0 cm, and the separation between Green and Blue gratings was 11.6 cm.

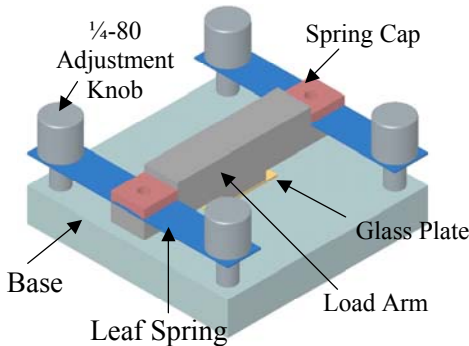


Figure 3. Transverse Load Fixture

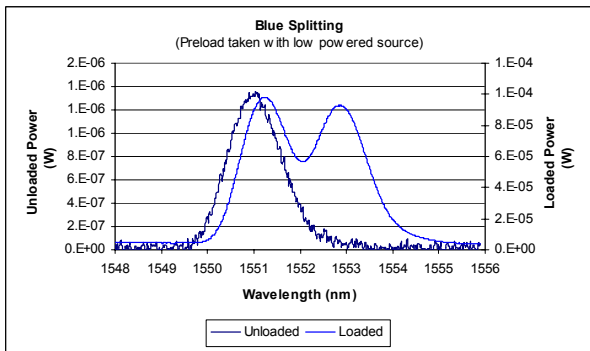


Figure 4. Reflection Spectra of Gratings Initial and loaded reflection spectra of gratings “Blue”.

The OFDR tunable laser system configuration is shown in Figure 5. Light from the scanning laser is split into three separate paths. The middle path passes the light

through a Hydrogen Cyanide (HCN) absorption cell, which is used as an absolute spectral reference. The upper path passes the laser light into a Michelson reference interferometer with arm length separation set at 5.4 cm, which results in an oscillation frequency of 10.5 kHz. The reference Michelson interferometer produces fringes which tend to drift in phase over time, but which provide a relative wavelength reference in between the HCN absorption peaks. These two references can be used to determine the scan position with approximately 0.001 nm accuracy. The lower path routes light to a Michelson interferometer with the transversely loaded fiber gratings in one arm and with cleaved bare fiber reference reflector (4% reflectivity) in the other arm. The length of the reference reflector arm is adjusted so that the reflector distance to the beam splitter is within 10 cm of the distance from the beam splitter to gratings Green and Blue. The limited coherence length did not permit us to observe grating Red with the reference reflector in this position, so after several scans were taken at the original reference arm length, the reference arm was shortened by 35 cm and re-cleaved so that grating Red could be measured as well. Each detector signal was amplified and passed into a 12-bit a/d circuit. The full width at half maximum of the grating peaks in the frequency domain was 200 Hz, corresponding to a physical width of 1.0 mm. This width indicates the spatial resolution to which we were able to measure the grating position. After obtaining the frequencies corresponding to each grating, the raw grating interferometer signal was passed through virtual eighth-order Butterworth band pass filters with widths of 600 Hz at the center frequencies corresponding to each grating. The absolute value of the filtered fringe patterns were calculated and averaged over 10 successive sweeps to obtain the fringe envelope function.

Comparisons between the loaded grating spectra taken by the OSA and by the OFDR technique (shown in Figure 6) show that the OFDR technique was successful in separating out the three grating spectra. There is some drift in peak position, but this is not entirely unexpected since a full week separated the measurements and the polyimide coating was certain to experience some non-elastic deformation that drifted slightly with time.

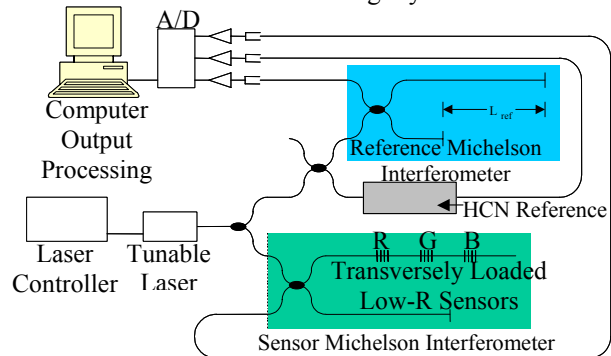


Figure 5. System Diagram of the Low Reflectivity Scanning Laser Demonstration

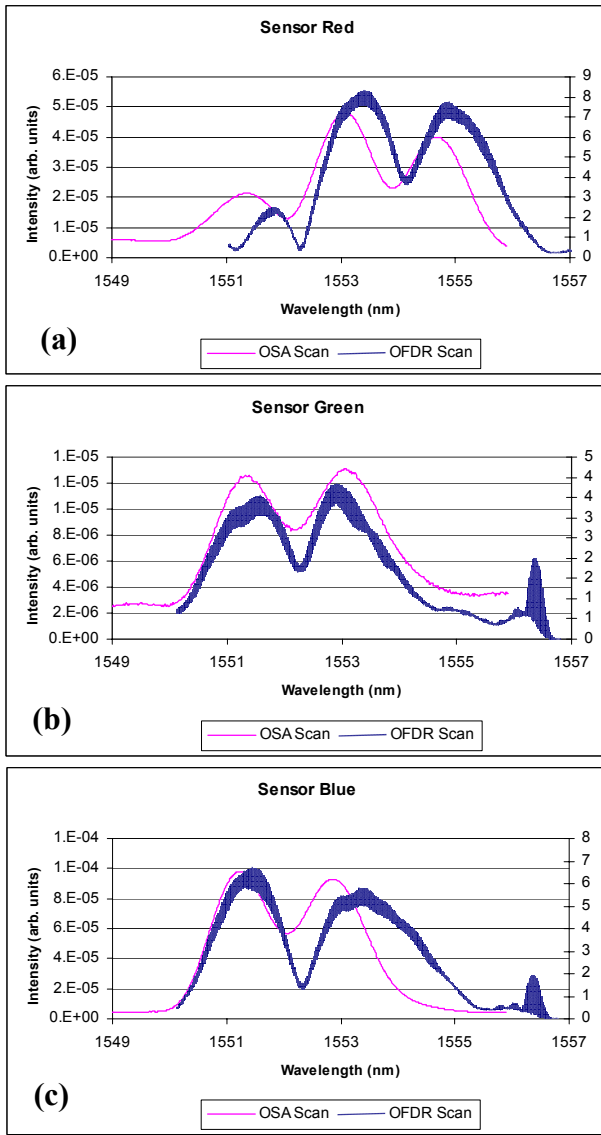


Figure 6. Comparison between Grating Reflection Spectra Obtained Directly From an OSA, and Spectra Obtained Using the OFDR Method One Week Later for Gratings a) Red, b) Green, and c) Blue

CONCLUSION

In summary we demonstrated that the Optical Frequency Domain Reflectometry technique could successfully discriminate between three overlapping transversely strained gratings despite their large differences in peak reflectivity. We also demonstrated the viability of using gratings written through the polyimide coating directly onto the fiber to make multi-axis strain measurements with a spatial resolution of 1 mm. This fabrication technique is a far more flexible, rugged, and cheaper alternative to traditionally written gratings. In addition we built a tunable laser with 0.8 mW output power and with very flexible scanning capabilities that include

tuning over a 40 nm range at over 100 Hz rates, and tuning over a 10 nm range (corresponding to a range of roughly 10,000 axial microstrain or 45,000 microstrain in a transverse direction) at rates close to 1000 Hz. This scanning flexibility will allow us the option to trade off length of the sensor string versus sampling rate in order to permit dynamic measurements over a limited length of fiber, with the limiting factor being the speed of the a/d data acquisition electronics. We also constructed a measurement system with a highly accurate dual HCN / interferometric wavelength references. Our ability to observe multi-axis gratings simultaneously over a greater physical range was limited by the short coherence length of the laser, but the simple replacement of the tuning element and the output coupler should dramatically enhance the coherence length for future demonstrations.

Acknowledgements

This work was funded by the US Air Force under contract number F33615-02-M-5601.

References

1. M. Froggatt and J. Moore, "Distributed Measurement of Static Strain in an Optical Fiber with Multiple Bragg gratings at Nominally Equal Wavelengths", *Applied Optics*, Vol. 37, p. 1741, 1998.
2. M. Froggatt and J. Moore, "High Spatial Resolution Distributed Strain Measurement in Optical Fiber with Rayleigh Scatter", *Applied Optics*, Vol. 37, p. 1735, 1998.
3. M. Froggatt, "Distributed Measurement of the Complex Modulation of a Photoinduced Bragg Grating in an Optical Fiber", *Applied Optics*, Vol. 35, p. 5162, 1996.
4. E. Udd, W.L. Schulz, J.M. Seim, E. Haugse, A. Trego, P.E. Johnson, T.E. Bennett, D.V. Nelson, A. Makino, "Multidimensional Strain Field Measurements using Fiber Optic Grating Sensors", *SPIE Proceedings*, Vol. 3986, p. 254, 2000
5. E. Udd, W.L. Schulz, J.M. Seim, A. Trego, E. Haugse, P.E. Johnson, "Use of Transversely Loaded Fiber Grating Strain Sensors for Aerospace Applications", *SPIE Proceedings*, Vol. 3994, p. 96, 2000.
6. T. Yamate, R.T. Ramos, R.J. Schroeder, E. Udd, "Thermally Insensitive Pressure Measurements up to 300 degree C using Fiber Bragg Gratings Written onto Side Hole Single Mode Fiber", *SPIE Proceedings*, Vol. 4185, p. 628, 2000
7. A. Trego, E. Haugse, E. Udd, "Material Removal Rate Fiber Optic Corrosion Sensor", *SPIE Proceedings*, Vol. 3489, p. 105, 1998
8. S. Yamashita, and M. Nishihara, "Widely Tunable Erbium-Doped Fiber Ring Laser Covering Both C-Band and L-Band," *IEEE Quantum Electronics*, Vol. 7, No. 1, pp. 41-43, 2001.
9. S. K. Kim, H. K. Kim, and B. Y. Kim, "Er-Doped Fiber Ring Laser for Gyroscope Applications," *Optics Letters* 19, 22, pp.1810-1812, 1994.
10. T. Plant, M. Winz, Oregon State Univ., to be published.